detritus | Multidisciplinary Journal for Circular Economy and Sustainable Management of Residues

CISA

TRUCK TYRE CHARACTERISATION AND KINETIC MECHANISM STUDY FOR VALUABLE CHEMICALS PRODUCTION

Maxwell Katambwa Mwelwa [1], Samuel Ayodele Iwarere [2,*] and Ntandoyenkosi Malusi Mkhize [1]

[1] *Chemical Engineering Discipline, University of KwaZulu-Natal, Durban 4041, South Africa*
[2] *Department of Chemical Engineering, Faculty of Engineering, Built Environment and Information Technology, University of Pretoria, Pretoria 0028, South Africa*

Article Info:
Received:
30 January 2025
Revised:
7 July 2025
Accepted:
6 August 2025
Available online:
9 September 2025

Keywords:
Truck tyre
Pyrolysis
Modelling
Py-GC/MS
Kinetic mechanism

ABSTRACT

Waste tyre pyrolysis is a promising strategy for converting end-of-life tyres into valuable chemical feedstocks. This study investigates the thermal degradation behaviour of truck tyre (TT) crumbs and evaluates the selective production of high-value compounds, particularly limonene and indene, under varying pyrolysis conditions. A combined approach employing thermogravimetric analysis, kinetic modelling (both model-free and model-fitting methods), and analytical pyrolysis coupled with gas chromatography-mass spectrometry (Py-GC/MS) was used to elucidate the relationship between temperature, heating rate, and product selectivity. Activation energy estimates ranged from 122 to 145 kJ.mol^{-1} across different kinetic models, indicating a multi-step degradation mechanism. The highest limonene selectivity (64.2%) was achieved at 400°C, but this declined to 28.5% at 700°C due to secondary cracking and aromatisation reactions. Additionally, faster heating rates enhanced limonene yield, with selectivity increasing from 30.8% at 20°C/min to 42.7% at 100°C/min. These results highlight the importance of optimising thermal parameters to favour the formation of target chemicals and provide essential kinetic and chemical data for the design of tyre pyrolysis systems focussed on selective product recovery.

1. INTRODUCTION

The depletion of natural resources and the need to minimise solid waste in metropolitan areas have necessitated the incorporation of used materials, especially waste tyres (WT), into manufacturing processes to valorise this form of garbage while reducing natural resources. As a result, techniques and recycling methods have been established to use tyres as feedstock for marketable products due to their high calorific value and a significant amount of carbon black. Among several techniques, pyrolysis has emerged as the most appealing for treating WTs (Mwelwa et al., 2023).

Pyrolysis is a feasible method for recovering valuable materials from waste tyre; however, commercial viability remains a challenge (Quek & Balasubramanian, 2012). In response, researchers have extensively studied its kinetics and mechanisms, predominantly using thermogravimetric analysis (TGA) to develop mathematical models that describe the thermal decomposition process. For instance, Williams and Besler (1995) correlated TGA profiles of different tyres with those of three rubber compounds (NR, BR, and SBR), enabling the extraction of kinetic parameters using Arrhenius-based models. Similarly, Seidelt et al. (2006) identified the main tyre constituents and superposed their DTG curves onto experimental tyre data to validate component-specific kinetics. While these approaches offered valuable insights into thermal degradation, they lacked the resolution to fully capture the chemical complexity of the pyrolysis vapour phase.

Han et al. (2018) used a thermogravimetric analyser in conjunction with a mass spectrometer to further understand the mechanism of WT pyrolysis. They discovered that WT pyrolysis DTG curves featured a bimodal peak between 250 and 500°C, and a modest peak between 600 and 800°C. In addition, the development of gaseous products detected using a mass spectrometer and the functional groups on the surface of the residue char detected with a Fourier-transform infrared (FTIR) spectrometer indicated that tyre pyrolysis could be partitioned into four different stages. The first stage occurred when the temperature was below 320°C, and at this stage, only minor mass was lost due to water vaporisation and plasticiser. The second stage is associated with the weight loss in the temperature range of 320 and 400°C and was attributed to the decom-

* Corresponding author:
Samuel Ayodele Iwarere
email: samuel.iwarere@up.ac.za

Detritus / Volume 32 - 2025 / pages 43-55
https://doi.org/10.31025/2611-4135/2025.19518

position of natural rubber. The third stage took place when the temperature was between 400 and 520°C and was attributed to the decomposition of synthetic rubber, while the fourth stage started when the temperature was above 520°C and was associated with little weight loss. Using the Master Plots method, Aslan et al. (2017) probed the most appropriate reaction model for waste tyre pyrolysis. Isoconversional methods were used to determine the averaged activation energy of 162.8 ± 23.2 kJ.mol^{-1} throughout a mass fraction conversion interval of 0.20 to 0.80. The reaction order of three was found to describe the pyrolytic decomposition better.

These earlier studies primarily emphasised devolatilisation, with limited focus on the formation of specific compounds. As a result, they offer minimal insight into how operational parameters such as temperature and heating rate influence the yields of target chemicals like limonene or indene, an aspect critical for optimising tyre pyrolysis for chemical and economic viability.

Recent efforts have shifted toward optimising pyrolysis parameters and modelling product-specific kinetics. Ngxangxa (2016) employed the qualitative and quantitative gas chromatography-mass spectrometric (GC-MS) and comprehensive two-dimensional gas chromatography (GC×GC) approaches to identify market-value compounds in tyre-derived oils (TDOs), including dl-limonene, p-cymene, benzothiazole, ethylbenzene, toluene, p-xylene, 3-ethyl toluene and α-terpinolene. Mkhize et al. (2019) further demonstrated that increasing heating rates influenced the synthesis of isoprene and dl-limonene, with higher rates favouring limonene production. Using the Kissinger method, they estimated activation energies of 133 and 115 kJ.mol^{-1} for isoprene and dl-limonene, respectively.

More recently, Menares et al. (2020) published a paper on fast WT pyrolysis using quasi-isothermal thermogravimetric analysis, kinetic modelling and an analytical pyrolyser with gas chromatography/mass spectrometry (Py-GC/MS). They found that devolatilisation/condensation and depropagation processes characterise WTs pyrolysis up to 482°C, while cyclisation and aromatisation of primary products create predominantly monoaromatics at higher temperatures. Isoprene (20.5%) and limonene (51%) were the most common chemicals found at temperatures below 500°C. Monoaromatics and gases were formed more readily at higher temperatures (over 600°C), with the equilibrated Diels-Alder reaction governing limonene and isoprene composition. Furthermore, the model-based and isoconversional approaches yielded kinetic parameters in high agreement (101-176 kJ.mol^{-1}). These studies highlight the importance of tracking chemical selectivity rather than just mass loss.

Despite the various studies on the thermochemical treatment of WT, data on the tracking of chemical formation remain scarce. Available literature still lacks comprehensive kinetic and mechanistic studies that integrate TGA-based models with Py-GCMS to simultaneously capture thermal and chemical evolution. Particularly scarce are studies that analyse the effect of both temperature and heating rate on the selectivity of key pyrolysis products by simultaneously applying both model-free/model-fitting kinetic analysis with chemical-specific Py-GC/MS tracking, as is done in this work.

The present study systematically investigates the pyrolysis behaviour of truck tyre (TT) with the goal of enhancing the selective recovery of valuable chemical compounds, notably limonene and indene. Unlike traditional approaches that primarily monitor devolatilisation behaviour through mass loss data, this study integrates advanced thermogravimetric modelling with dual-mode analytical pyrolysis-gas chromatography/mass spectrometry under both single-shot and EGA modes to assess how temperature and heating rate directly affect the selectivity of the target products. The combined use of model-free and model-fitting kinetic analyses addresses the complexity and multi-step nature of waste tyre pyrolysis. Model-free methods, such as Friedman and Starink, offer conversion-dependent activation energy estimates without the need to assume a specific reaction mechanism, making them robust for heterogeneous reactions. Meanwhile, model-fitting approaches like the Coats-Redfern method facilitate mechanistic interpretation by aligning experimental data with theoretical kinetic models. When coupled with compound-specific Py-GC/MS analysis, which enables precise identification and quantification of key pyrolysis products, this approach provides both thermal and molecular-level insights into reaction pathways. This integrated methodology offers a powerful framework for evaluating the influence of temperature and heating rate on product selectivity, ultimately contributing to improved process optimisation and the potential design of efficient tyre pyrolysis systems geared toward chemical valorisation.

2. MATERIALS AND METHODS

2.1 Feedstock compositional analysis

Truck Tyre (TT) crumbs samples of particle size less than 1 mm (maximum particle size), obtained from a local tyre recycler and stored in airtight plastic bags, were used for all experiments conducted in this study. The proximate analysis was carried out using a thermogravimetric analyser (TA 60WS, Shimadzu, Japan) and computations using a slightly modified ASTM E 1131-08 (2008). The maximum temperature was set to 800°C to determine the mass loss as temperature increases and nitrogen was used as an inert medium to purge hot volatiles at a low heating rate (10°C/min) before switching to oxygen, the combusting/oxidising medium. The ultimate analysis was conducted using the Leco analyser (SC632, Leco, United States) to evaluate the C, H, N, and S quantities in the analytical TT. For CO_2 and SO_2 formation, a sample of 0.5 mm was combusted into pure O_2, followed by detection and quantification by infrared detection. The higher heating value of the sample (HHV) was calculated using the Boiés correlation (Han et al., 2017) for polymeric materials and biomass. Finally, the organic compounds in TT crumbs were investigated using a Fourier transformed infra-red (FT-IR) spectrometer (Prestige-21, Shimadzu, Japan) integrated with a platinum attenuated total reflection (ATR) single-reflection module. The samples' spectra were aggregated from 32 scans with a

resolution of 4 cm^{-1} in the 400-4000 cm^{-1} range, and data were analysed using LabSolutions IR software.

2.2 Thermogravimetric analysis

Thermogravimetric analysis (TGA) was applied to investigate the thermal degradation behaviour of the TT. A tyre crumbs sample of (10±1) mg was used in all tests, with a single repetition. A thermobalance (TA 60WS, Shimadzu, Japan) was used to record weight loss as a function of temperature from 30 to 800°C. Experiments were conducted in triplicate under identical operating conditions, at several heating rates (10, 20, 30, 40 and 50°C/min) and making use of the same carrier gas N_2 (99.99% pure) at the rate of 100 mL/min. The resulting thermogravimetric (TG) and derivative thermogravimetric (DTG) curves from the three runs exhibited similar thermal degradation trends.

2.3 Kinetic analysis

The linear mathematical analysis methods allow the estimation of the kinetic parameters such as the activation energy and the pre-exponential factor by establishing linear relationships between the kinetic parameters, using mass loss information collected at multiple devolatilisation rates.

The rate of a solid-state reaction in its most general form is depicted by the following equation:

$$\frac{d\alpha}{dt} = k(T)\, f(\alpha) \quad (1)$$

where k represents the reaction rate constant, f(α) the reaction model, and α the conversion fraction.

The conversion percent at any particular time in isothermal thermogravimetric analysis, given by:

$$\alpha = \frac{m_0 - m_t}{m_0 - m_\infty} \quad (2)$$

with m_0 the initial sample weight, m_t the sample weight at time t, and m_∞ the final sample weight.

In non-isothermal thermogravimetric analysis, the conversion fraction at a given temperature is:

$$\alpha = \frac{m_0 - m_T}{m_0 - m_\infty} \quad (3)$$

where: m_T represents the weight of the sample at temperature T.

The integral rate law is obtained by integrating the above equation Equation (1),

$$g(\alpha) = kt \quad (4)$$

where: g(α) is the integral model of degradation.

The temperature dependence of the rate constant is described by the following Arrhenius equation,

$$k = Ae^{-E_a/RT} \quad (5)$$

where: A represents the pre-exponential factor, Ea the activation energy, T the absolute temperature, and R the gas constant.

The substitution of Equation (5) into rate law equations gives,

$$\frac{d\alpha}{dt} = Ae^{-E_a/RT}\, f(\alpha) \quad (6)$$

And,

$$g(\alpha) = Ae^{-E_a/RT} t \quad (7)$$

The following equation can be used to convert Equations (6) and (7) into non-isothermal rate equations that express reaction rates as a function of temperature at a fixed heating rate:

$$\frac{d\alpha}{dT} = \frac{d\alpha}{dt} \cdot \frac{dt}{dT} \quad (8)$$

where: dα/dT is the non-isothermal reaction rate, dα/dt the isothermal reaction rate, and dT/dt the heating rate (β).

The differential formulation of the non-isothermal rate law is obtained by substituting Equation (6) into the preceding equation.

$$\frac{d\alpha}{dT} = \frac{A}{\beta} e^{-E_a/RT} f(\alpha) \quad (9)$$

Upon integration, Equation (9) gives,

$$g(\alpha) = \frac{A}{\beta} \int_0^T e^{-E_a/RT}\, dT \quad (10)$$

This study employed both model-free and model-fitting kinetic approaches to rigorously investigate the thermal decomposition behaviour of TT pyrolysis. The adoption of this hybrid methodology lies in the inherent complexity and heterogeneity of waste tyre materials, which undergo multi-phase and multistep decomposition processes involving overlapping primary and secondary reactions. Model-free methods (Friedman, Kissinger, and Starink) were selected for their capability to estimate the apparent activation energy (E_a) as a function of conversion (α) without requiring a predefined reaction mechanism. This feature makes them particularly well-suited for analysing systems where the reaction pathway is not singular or where multiple overlapping mechanisms occur, as is characteristic of polymeric solid waste pyrolysis.

In contrast, model-fitting methods such as Coats-Redfern and the Differential method require the assumption of a specific reaction model but offer insights into the likely reaction mechanism when the best-fitting model function is identified through statistical criteria (e.g., R^2). The Coats-Redfern method, in particular, is widely used due to its mathematical simplicity and effectiveness in evaluating single-step approximations of complex reactions. The application of the differential method further allows for fine-resolution analysis at discrete temperature intervals, adding robustness to the kinetic interpretation.

Combining these two methodological paradigms ensures a comprehensive kinetic assessment: model-free methods offer mechanistic neutrality and robustness across conversion ranges, while model-fitting approaches facilitate mechanistic hypothesis testing and validation. This multi-method strategy enhances the reliability and interpretive depth of the kinetic parameters derived (Seidelt et al., 2006; Starink, 2003; Vyazovkin et al., 2011). Importantly, this integrated approach provides not only activation energies but also mechanistic insights, which are essential for the design and optimisation of pyrolysis processes aimed at selective recovery of valuable compounds such as limonene and indene.

The direct differential technique employs the differential formulation of the non-isothermal rate law. By considering the logarithm form of the non-isothermal rate law, the general expression of this method is given by Equation (11) below. The activation energy (E_a) and pre-exponential fac-

tor (k0) are obtained from the slope of ln dα/dT/f(α) versus 1/T (Khawam & Flanagan, 2006).

$$\ln\frac{d\alpha/dT}{f(\alpha)} = \ln\frac{k_0}{\beta} - \frac{E_a}{RT} \quad (11)$$

with f(α) the reaction model, α the conversion fraction, T the temperature, Δα and ΔT their respective incremental differences, dα/dT the non-isothermal reaction rate, R the gas constant and β the heating rate.

The Coats-Redfern method uses the integral form of the non-isothermal rate law and its approximation. The mathematical assumption of this method corresponds to a zero-order reaction, and its general equation is given by Equation (12) below. The E_a and k_0 are obtained from the slop of ln $g(\alpha)/T^2$ versus 1/T (Coats & Redfern, 1965; Khawam & Flanagan, 2006).

$$\ln\frac{g(\alpha)}{T^2} = \ln\left(\frac{k_0 R}{\beta E_a}\left[1 - \left(\frac{2RT_{exp}}{E_a}\right)\right]\right) - \frac{E_a}{RT} \quad (12)$$

where g(α) represents the integral decomposition model, β the heating rate and T_{exp} the mean experimental temperature.

The Friedman's isoconversional approach is based on a comparison of tests conducted at various linear heating rates. It works with varying conversion degrees by using the logarithm of conversion rate as a function of inverse temperature (Friedman, 1964; Venkatesh et al., 2013). The mathematical form of this method is given by Equation (13). The Kinetic parameters are obtained from the plot of ln (β dα/dt) against 1/T, with dα/dt the isothermal reaction rate.

$$\ln\frac{g(\alpha)}{T^2} = \ln\left(\frac{k_0 R}{\beta E_a}\left[1 - \left(\frac{2RT_{exp}}{E_a}\right)\right]\right) - \frac{E_a}{RT} \quad (13)$$

The Kissinger method is based on determining the temperature at the highest devolatilisation rate at different heating rates (Kissinger, 1957). The mathematical form of the Kissinger method is given by Equation (14). In this method, E_a and k_0 are obtained from the slope of ln (β/T_m^2) versus 1/T, Tm is the temperature at which the maximum rate occurs.

$$\ln\left(\frac{\beta}{T_m^2}\right) = \ln\left(\frac{k_0 R}{f(\alpha)}\right) - \frac{E_a}{RT_m} \quad (14)$$

The Starink's method combines the Flynn-Wall-Ozawa (FWO) and Kissinger-Akira-Sunose (KAS) isoconversional methods into a single expression (Starink, 2003) given by Equation (15). In this expression, C_s is a constant factor that is irrespective of β and T. The Starink's activation energy and pre-exponential factor are calculated from the slop of ln $(\beta/T^{1.8})$ against 1/T.

$$\ln\left(\frac{\beta}{T^{1.8}}\right) = C_s - 1.0037\left(\frac{E_a}{RT}\right) \quad (15)$$

2.4 Pyrolysis coupled with mass spectrometry (Py-GC/MS)

The pyrolysis was performed in a multi-shot pyrolyser (EGA/PY-3030D, Frontier Laboratories Ltd., Japan) based on a proprietary, high-temperature-resistant ceramic heater with low heat capacity. The system consists of the pyrolyser furnace, which also serves as a thermal desorption unit, and a temperature controller. The multi-shot pyrolyser is coupled with the GC/MS equipment, which comprises a gas chromatograph combined with a mass spectrometer to separate, categorise and measure sophisticated polymeric materials.

This study used a multi-shot pyrolyser EGA/PY-3030D interfaced with a gas chromatograph (GC-2010 Plus, Shimadzu, Japan) with the AOC-20I auto-injector, fitted with a MS detector (QP 2010 Ultra, Shimadzu, Japan). In all the tests, the interface line remained fixed at 250°C, and the volatile compounds were carried out of the pyrolysis reactor using a regular air flow of 54.1 mL/min. 1±02 mg of TT sample were loaded into a sample holder (Frontier Laboratories Eco-cup SF, 50 µL) and inserted into the oven using an auto-shot sampler.

The products of pyrolysis (1:50 split ratio) were isolated in a Zebron capillary GC column (ZB-5MS) of 30 m length, 0.25 mm internal diameter and 0.25 µm film thickness, and were analysed in a mass spectrometer sensor (70 eV ionisation) in the m/z range of 30-800. The carrier gas was made up of 99.99% pure helium.

Two separate analytical procedures were applied, namely single-shot and evolved gas analysis (EGA). The single-shot experiments have been conducted to investigate the effect of temperature on the chemical production and, therefore, determine the optimal pyrolysis temperature. Based on data from the thermogravimetric analysis, tests were carried out at various temperatures (400, 500, 600, and 700°C). Chromatograms were analysed regarding the peak area% of two marketable chemicals, i.e., limonene and indene. The EGA experiments, however, have been conducted at various heating rates considered in the kinetics study (10, 20, 30, 40 and 50°C /min) to investigate the effect of heating rate at the optimal temperature. A difference in split ratios (96 for single-shot vs. 50 for EGA) was used to balance signal intensity and resolution. A lower split ratio in EGA mode ensures sufficient detection sensitivity over extended heating rate ranges, while a higher split ratio in single-shot mode prevents detector saturation at higher analyte concentrations during fixed-temperature runs. All analyses were performed in triplicate to confirm the reproducibility of the chemical composition profiles. The chromatographic profiles obtained from the replicate runs displayed consistent retention times and relative peak intensities for major compounds.

Product quantification was carried out on a relative basis from the total ion chromatograms (TIC) obtained by the Py-GC/MS system. Compounds were identified through the National Institute of Standards and Technology (NIST) library matching and confirmed by characteristic retention times.

The data from the Py-GC/MS analysis were analysed using the selectivity to a specific species S_i, defined as the proportion of an ith- chromatographic compound's peak ($PArea_i$) to the aggregate of all detected peak areas ($\sum PArea_i$) and given by Equation (16). Additionally, the factor $\xi_{a\text{-}b}$ was employed to assess the relative production of relevant compounds, Equation (17) (Menares et al., 2020).

$$S_i = 100\,x\left(PArea_i \Big/ \sum_{i=1}^{n} PArea_i\right) \quad (16)$$

$$\xi_{a-b} = (S_a/S_b) \quad (17)$$

With:
S_i, the selectivity to a specific specie or compound ,
$PArea_i$, the chromatographic peak of an ith compound,
$\sum_{i=1}^{n} PArea_i$ the aggregate of all detected peak areas,
$\xi_{a\text{-}b}$, a quantifier of a and b compounds relative formation
a, b, the produced compounds such as limonene, etc.

3. RESULTS AND DISCUSSION

3.1 Compositional characterisation

The process of tyre decomposition and the final composition of the volatile products from tyre pyrolysis are affected by waste tyre properties or composition. These components are identified via proximate and ultimate investigations that allow for the estimation of the pyrolysis opportunities of WTs. Table 1 summarises the proximate and ultimate analysis data.

The reported high content of volatile matter (60.8%) indicates that the studied material is pyrolysable. The results in Table 1 are consistent with many of those previously published on waste tyres, which range from 58 to 66% for the volatile matter, 27.5 to 32% for the fixed carbon and 4.2 to 5.4% for the ash content (Iwarere & Mkhize, 2019; Li et al., 2004; Menares et al., 2020; Roy & Unsworth, 1989; Tsipa et al., 2024). The high carbon content of the investigated material indicates that it is a promising source of energy, whether through direct combustion or as a raw material for the generation of liquid fuels. The estimated higher heating value (HHV) matched that reported by previous research (Li et al., 2004; Menares et al., 2020).

The FTIR spectrum of the sample (Figure 1) presented two characteristic bands at 2915 and 2846 cm^{-1}, which are commonly linked to -CH- asymmetric stretching vibrations of $-CH_3$ and $-CH_2-$ chemical groups and, to the -C-H symmetric stretching vibrations of the same chemical groups. Nunes et al. (2008) associated the two bands to be characteristic of the spectrum of natural rubber. Besides the two bands, three other characteristic vibrational signals were observed at around 1537, 1438 and 1373 cm^{-1}. These absorbance peaks respectively showed the stretching of C-H, C-C and C-N functional groups, related to the Synthetic rubber (SBR and BR) (Khan et al., 2017, Nunes et al., 2018).

TABLE 1: Waste truck tyre compositional analysis.

Proximate analysis (wt.%)		Standard deviation (σ)
Moisture	3,4	0.17
Volatile Matter	60,8	3.04
Fixed Carbon	31,8	1.59
Ash	5,3	0.27
HHV (MJ/kg)	34,12	1.71
Ultimate Analysis (wt.%)		**Standard deviation (σ)**
C	77,9	3.90
H	6,6	0.33
N	0,5	0.03
S	2,8	0.14
O	6,8	0.34

3.2 Thermogravimetric analysis (TGA)

The profiles of the thermogravimetric analysis based on the pyrolysis temperature at five heating rates are illustrated in Figure 2.a. It is observed from Figure 2.a that although the mass loss of TT appears to begin at about 200°C, the rate of mass loss stays modest until 300°C, when the tyre devolatilisation becomes considerably more rapid until the final temperatures are reached. The final or terminal temperature is illustrated by graphs appearing to reach a plateau at various heating rates and estimated at 500-600°C for the experimental tyre.

The thermogravimetric profiles reveal that irrespective of the heating rate, the shapes converge to the same solid residual value at the end of pyrolysis. The stated char values are the aggregate of the fixed carbon and ash contents observed during proximate analysis and are based on an

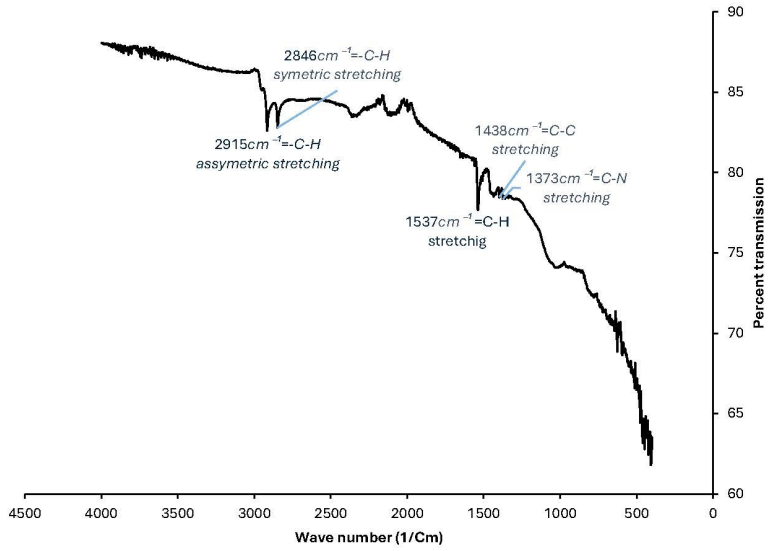

FIGURE 1: Truck tyre FTIR spectrum.

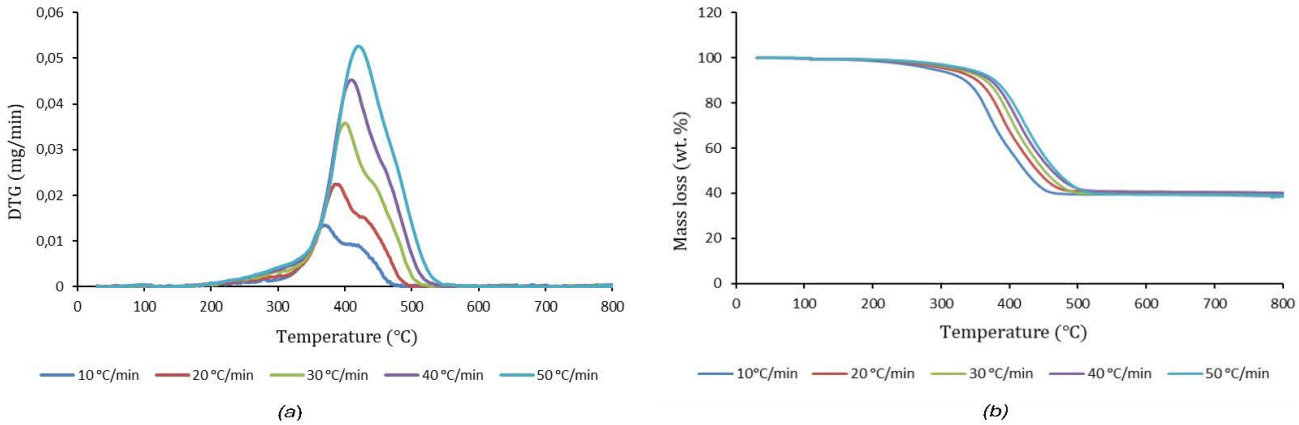

FIGURE 2: a. TGA and b. DTG curves derived from the thermogravimetric analysis of TT.

average of all the heating rates (10 to 50°C/min). The observed char residual, 38.7 wt.%, is comparable to the previously reported work (Menares et al., 2020).

The DTG profile at heating rate β=20°C min illustrated in Figure 2.b, presents a prominent devolatilisation peak around 378,9°C associated with the thermal breakdown of NR via β-scission, and a shoulder at 433,7°C associated with SBR decomposition and styrene evolution; which are comparable to those reported in previous work at the similar heating rate (Menares et al., 2020). These two peaks have long been thought to be characteristic of polyisoprene rubbers (Danon & Görgens, 2015). When the heating rate increases, the prominent peak increases while the shoulder disappears. This phenomenon has been linked to the reduction of second reactions at higher heating rates with a promotion of the rubbers' devolatilisation (Danon et al., 2015). Devolatilisation/condensation reactions at moderate temperatures are more likely to produce condensation compounds, which then fragment and reorganise to produce pyrolysis products, according to several studies (Mkhize et al., 2016; Xu et al., 2018). Furthermore, at lower temperatures, the primary devolatilisation peak has been linked to the decomposition of polyisoprene and, to less extent, styrene-butadiene rubber. Hence, some alkenes such as limonene are abundant in the pyrolysis of hot volatiles at these lower temperatures (363.35°C at 10°C/min to 424.6°C at 50°C/min) (Danon et al., 2015; Mkhize et al., 2016).

The relationship between the heating rate and the devolatilisation reaction progress is depicted in Figure 3. The influence of the heating rate on the devolatilisation peak temperature is evidenced by a rise of temperature linked with the maximum devolatilisation rate as the heating rate rises.

3.3 Kinetic analysis

3.3.1 Model-free methods

The Friedman, Kissinger and Starink's methods were the model-free methods used to calculate the activation energy and pre-exponential factor. Linear regression graphs for these methods are plotted using Equations (13), (14) and (15), and their linear graphs are shown in Figures 4.a., c. and d., respectively.

The Friedman linear plots, represented in Figure 4, have an identical gradient, therefore the estimated activation en-

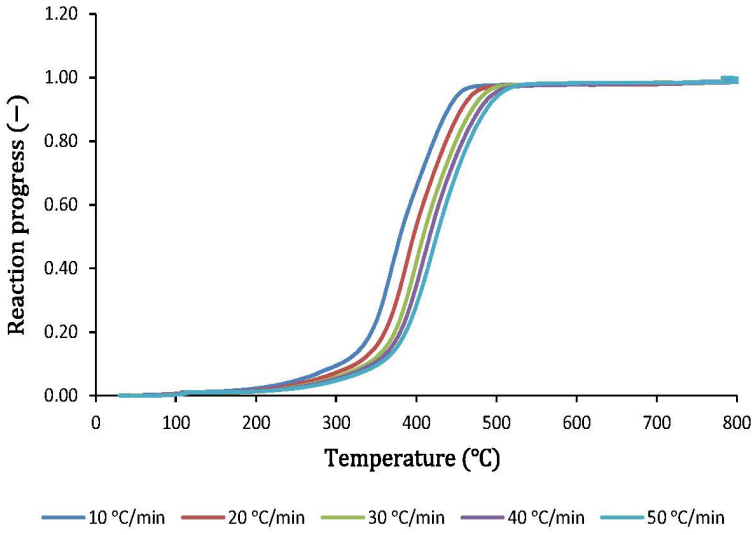

FIGURE 3: Reaction progress of the waste truck tyre.

ergy is irrespective of the reaction progress. Figure 5 presents the activation energies at various conversion rates, calculated from the gradient of different plots. Two sets of linear plots have been identified for the experimental TT, i.e., the first set from reaction progress of 0.1 to 0.4 with a maximum peak at reaction progress of 0.2 and the second set from reaction progress of 0.4 to 0.9 with the maximum peak at reaction progress of 0.7. As a result, the activation energy (E_a) as a measure of the reaction progress (α) reaches a maximum value of 139.04 kJ.mol^{-1} at reaction progress of 0.7. Iwarere and Mkhize (2019) also reported a maximum peak at reaction progress of 0.7 for truck tyres, with a similar estimation approach. Values of E_a obtained in the present study by the isoconversional Friedman method ranged from 105.5 to 139.04 kJ.mol^{-1} with an average estimated at 122.0 kJ.mol^{-1}. The pre-exponential factor (k_0) also presents a similar trend with an average k_0 estimated at 2E+08 s^{-1}.

The two peaks identified on the E_a vs α profile are associated to two pyrolysis process regions. The first region, between 343°C and 386°C is associated with the devolatilisation/condensation of NR and SBR. The allylic poly-isoprene molecules undergo depropagation and intramolecular cyclisation-scission in this zone, generating isoprene and limonene as hinted by Mkhize et al. (2016). The second region, between 392 and 437°C, could be linked to the scission and dehydrogenation of the SBR, which results in the synthesis of styrene and butadiene monomers. Menares et al. (2020) also reported the presence of two significant regions at 358-382°C and 387-433°C respectively.

The Kissinger method uses an integrated approach to determine activation energy (E_a) and pre-exponential factor (k_0). The E_a estimated using the Kissinger plots was 138.5 kwith a pre-exponential factor of 3E+05 s^{-1}. A difference between the E_a calculated from the Friedman method (average), and the Kissinger method is around 16.5 kJ.mol^{-1}. However, the value of E_a obtained with the present method is comparable to the maximum value of E_a estimated with the Friedman method at around 0.5 units of difference. The appearance of the shoulder on the profiles of the first derivative, which disappears as the heating rate rises, could explain the disparity in activation energy values. The absorption of the shoulder to the prominent peak affects the estimation of the E_a. In addition, the pre-exponential coefficient in the Friedman approach was shown to be greater than in the Kissinger approach.

Similar to the Kissinger method, Starink's method integrates into a single equation two iso-conversional techniques, i.e., the FWO and the KAS techniques. The estimated values of E_a and k_0 using this method, were 139.7 kJ.mol^{-1} and 1E+06 s^{-1}, respectively. The obtained E_a value falls in the range of those obtained by Menares et al. (2020)

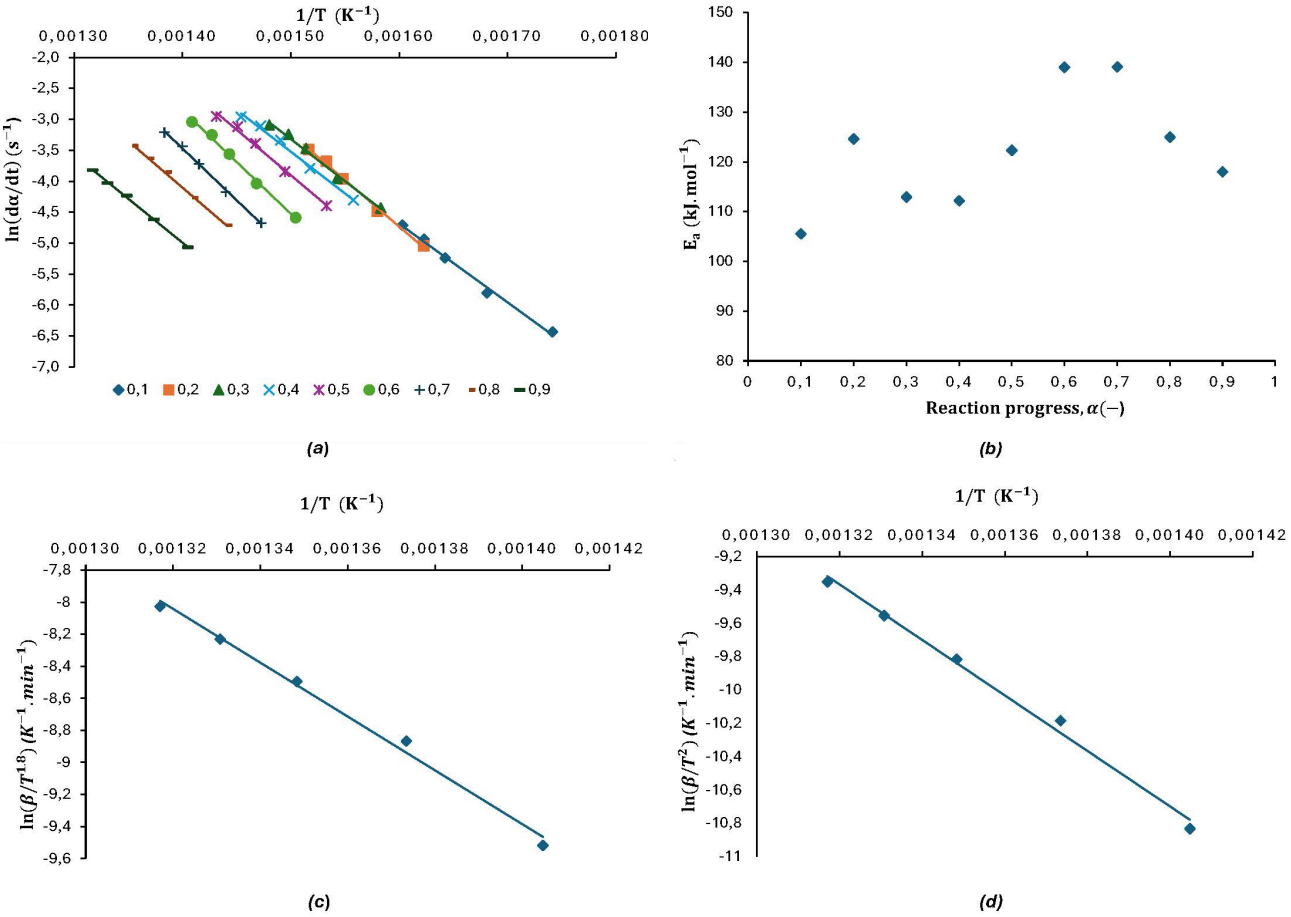

FIGURE 4: Model-free methods: a. Friedman method linear plots, b. Friedman activation energy vs reaction, c. Kissinger method linear plot, and d. Starink's method linear plot.

using a similar method. They reported values of E_a ranging from 101.5±2 to 176.7±2 kJ.mol^{-1}. The maximum values of E_a estimated with the model-free methods have slight differences, with the highest value obtained with Starink's approach. The same technique presented the highest pre-exponential factor.

3.3.2 Model-based methods

Two conventional methods, namely the direct differential and the Coats-Redfern methods, were used for five distinct heating rates (10, 20, 30, 40 and 50°C/min). For E_a and k_0 estimation, we fitted ten models in the two calculation methods. The used models were the first order (F1), the second-order (F2), the first diffusion (D1), the second diffusion (D2), the power low (P2), the power low (P3), the Avrami-Erofyev (A2) and (A3), the Prout-Tompkins (B1) and the contracting area (R2) models. For each method, the best-fitting model used to evaluate the kinetic parameters has a greater coefficient of determination R^2. The linear plots of the considered models for the two methods at 20°C/min are presented in Figures 5.a and b.

The E_a and K_0 were estimated for each considered model, and among all the considered models, the second-order and first diffusion models were considered the best fitting for respectively the Coats-Redfern (C&R) and differential method (Diff.), based on the higher coefficient determination R2 of 0.98 and 0.99, respectively. While the D2 and F2 models showed the best statistical fit based on R2 values, we acknowledge that pyrolysis is a multi-step and heterogeneous process involving overlapping reactions such as depolymerisation, cyclisation, and aromatisation. Therefore, the identified models should be viewed as approximations capturing dominant mechanisms under the tested conditions, not comprehensive descriptors of the entire process.

Using the differential method, E_a was estimated at 144.4 kJ.mol^{-1} while 128.3 kJ.mol^{-1} was found for Coats-Redfern approach. The respective pre-exponential factors k_0 were 1.6E+10 s^{-1} and 2.8E+03 s^{-1}.

A comparison of different activation energies estimated at various heating rates reveals an increase in activation energy as the heating rate rises. A similar trend was observed for the pre-exponential factor k_0 that tended to increase with the increase in the heating rate. These results are in good correlation with those reported by Leung and Wang (1998) while conducting a kinetic analysis of WT pyrolysis. The average E_a has been estimated respectively at 144.41 kJ.mol^{-1} and 130.60 kJ.mol^{-1} for the Differential method and the Coats-Redfern method. The respective obtained pre-exponential factor is 1.9E+10 s^{-1} and 3.7E+03 s^{-1}.

To assess the robustness and reliability of the derived kinetic parameters, each kinetic model applied in this study was subjected to linear regression analysis. The linear plots used to estimate activation energy from $\ln(g(\alpha)/T^2)$ versus 1/T (Coats-Redfern), or $\ln(\beta/T^2)$ versus 1/T (Kissinger, Starink), demonstrated excellent linearity, with correlation coefficients (R2) consistently exceeding 0.95. These high R2 values indicate a strong statistical fit between the experimental data and the kinetic model assumptions, validating the appropriateness of the chosen models for describing the pyrolysis of TT. In addition to R2 evaluation, the standard deviations of the calculated activation energies were estimated from the slope errors of the linear regressions. This provided a quantitative measure of variability and uncertainty associated with the E_a values obtained. These deviations ranged from ±3.2 to ±6.7 kJ.mol^{-1}, depending on the method used and the temperature interval considered. The relatively narrow error bands confirm that the reported activation energies are statistically significant and reproducible within the experimental design.

The different activation energies and pre-exponential factors estimated with the five considered approaches are summarised in Table 2.

The differential method provided the highest activation energy with a difference of about five units within the two model-free approaches of Kissinger and Starink. Friedman's and Coats-Redfern methods present the lower activation energy values with a significant difference of about 22 and 16 with the differential method. The estimated values of E_a derived from this study range between 122 and 145 kJ.mol^{-1}, depending on the kinetic method applied. These values are in strong agreement with those reported in the literature for waste tyre pyrolysis. For instance, Menares et al. (2020) reported E_a values between 101 and 176 kJ.mol^{-1} for fast pyrolysis of ground waste tyres, while Seidelt et al. (2006) Danon et al. (2015) report-

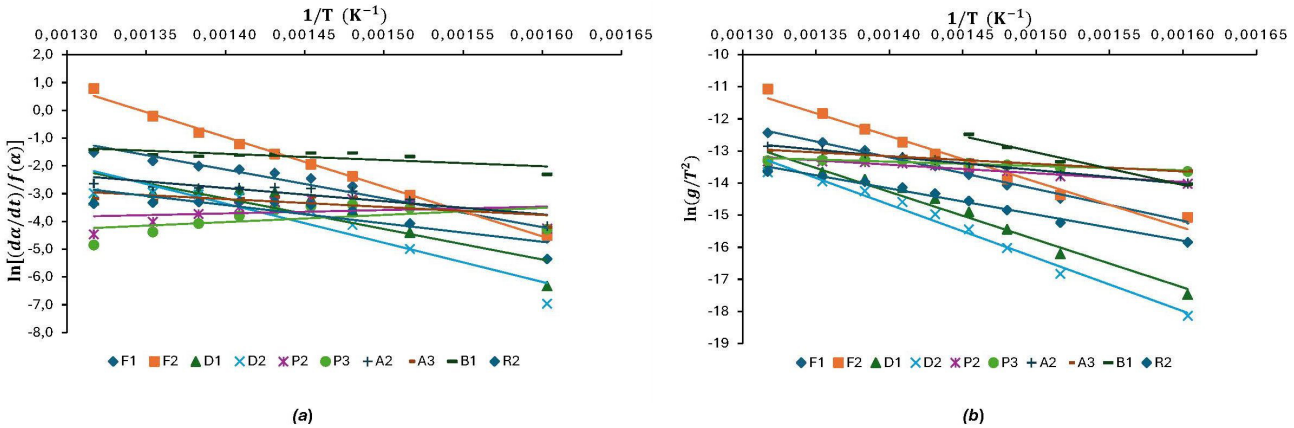

FIGURE 5: Model-based methods: a. Differential method linear plots and b. Coats-Redfern method linear plots.

TABLE 2: Kinetic parameters obtained with different methods.

Methods	Ea (kJ.mol^{-1})	k_0 (s^{-1})
Friedman	122.00	1.9E+08
Kissinger	138.46	3.0E+05
Starink	139.68	1.4E+06
Differential	144.41	1.9E+10
Coats-Redfern	130.60	3.7E+03

ed ranges of 143 to 254 kJ.mol^{-1} and 80 to 434 kJ.mol^{-1} respectively, depending on the heating rate and analytical technique. This consistency underscores the reliability and reproducibility of the kinetic data generated in this study, despite variations in experimental conditions and analytical models.

Notably, the highest E_a value obtained from the differential method (144 kJ.mol^{-1}), consistent with its sensitivity to early-stage decomposition, closely aligns with the maximum activation energies calculated via the model-free methods, particularly Kissinger and Starink, thereby demonstrating methodological convergence and internal robustness. The slight deviations observed among different methods are expected due to their inherent mathematical formulations and assumptions. Model-free methods estimate apparent activation energies across the full range of conversion without assuming a reaction model, while model-fitting techniques interpret data based on specific mechanistic functions.

Additionally, the variation in E_a values is also influenced by the complex composition of the feedstock. Truck tyres, like most commercial tyres, consist of a heterogeneous mixture of NR, SBR, carbon black, plasticisers, sulphur, and metallic additives. Each of these components decomposes over distinct temperature ranges and via different mechanisms, leading to overlapping thermal processes. This multicomponent nature results in broader activation energy distributions and can shift the average E_a evaluation depending on whether devolatilisation is dominated by NR, SBR, or secondary crosslink breakdown. These lower activation energies obtained in this study indicate that the process requires less energy and, therefore, does not necessarily require a catalyst for its completion.

3.4 Py-GC/MS

To match the TGA data and kinetic observations with the potential reaction pathways occurring in truck tyre pyrolysis, various Py-GC/MS tests were conducted. WTs pyrolysis is a technique with unique characteristics in terms of products distribution. Some variables, such as the heating rate and, most significantly, the reaction temperature, are critical in determining transport restrictions and reaction kinetics. To improve the selectivity of specific marketable chemicals, a detailed evaluation of WT pyrolysis variables is necessary.

3.4.1 Compound identification

The most abundant compounds identified among several chemicals form the TT pyrolysis are gases (alkanes, alkenes, COx and H_2), cyclic hydrocarbons (Cyclo-butene, cyclo-propane, limonene, isoprene and indene) and aromatics (xylene, benzene, and styrene). Aromatics are generated after a significant conversion cyclic compounds through aromatisation and hydrogenation, as observed by Ding et al. (2016).

From all the experiments conducted at different temperatures (400-700°C), two peaks were identified and are associated with isoprene and limonene. These two chemicals have a cumulative peak-based selectivity of about 40% below 600°C, which declines at temperatures of 600°C and above. The significant cumulative selectivity below 600°Cindicates that only minor cyclisation and aromatisation reactions occur in condensed molecules. The increase in temperature to 500°C and above led to the peak-based selectivity of benzene, toluene, xylene, styrene, and indene to increase from about 6% to 12% at 700°C. According to the findings, temperature emerges as the most important factor in the pyrolysis of truck tyres and dictates the kinetics and product distribution.

3.4.2 Temperature influence on chemical production

As observed in previous research, temperature is a major operating parameter in WT pyrolysis (Ding et al., 2015; Menares et al., 2020; Xu et al., 2018). This research examines two chemicals derived from TT during Py-GC/MS experiments and involves tests conducted at various temperatures. Figure 6 presents the temperature effect on the selectivity of significant chemicals.

The selectivity to limonene (S_l) appeared to continuously decay with the increase in temperature up to a minimum selectivity of 28.5% at 700°C. In contrast, the selectivity to indene (tends to be constant at 500 and 600°C (Table 3). The latter has been only detected at temperatures of 500 and 600°C, and the temperature has no major influence on the productivity of this compound in the considered range of temperatures. These results on indene productivity agree with those obtained by Li et al. (2004), who observed an increase in indene productivity at around 500°C before it tends to decrease at higher temperatures. However, the transition of limonene to alkenes under 600°C and the conversion of a fraction of limonene into monocyclic aromatics such as benzene, toluene and xylene can justify the drop in the selectivity to limonene. Isoprene, one of the significant compounds detected, shows a maximum at around 500°C. Therefore, 500°C emerged as optimal temperature. To better characterise the product distribution, a semi-quantitative analysis of the key compounds using normalised peak area integration of the Py-GC/MS chromatogram obtained at 500 , showed that limonene was the dominant compound, representing 49.9% of the total detected peak areas. Isoprene (37.6%) was the second most abundant. Indene (0.2%), toluene (3.0%), and styrene (4.2%) were also detected in smaller proportions, indicating secondary cracking and aromatisation reactions.

Several researchers have evidenced that isoprene and limonene are synthesised from natural rubber, via a sequence of β-scission and depropagation processes of NR and intramolecular cyclisation and scission of monomeric isoprene, respectively. Limonene is also synthesised from isoprene at higher temperatures through Diels-Alder re-

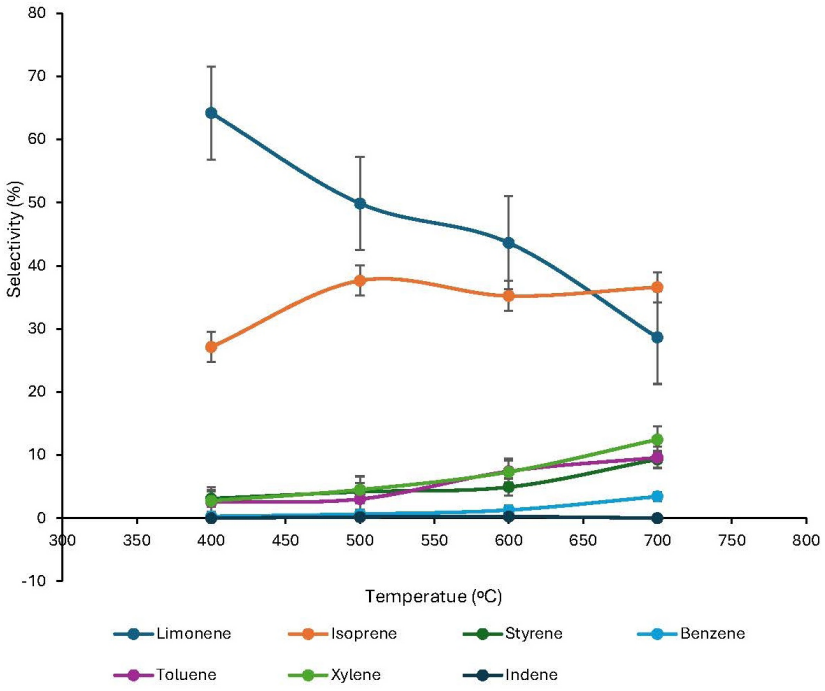

FIGURE 6: Selectivity to important compounds.

actions (Mkhize et al., 2016; Xu et al., 2018). On the other side, Doddipatla et al. (2021) proved that indene is formed via a bimolecular reaction involving the simplest organic radical methylidyne (CH) and styrene (C6H5C2H5) through the hitherto elusive methylidyne addition, cyclisation and aromatisation.

The relative formation of limonene to isoprene ($\xi_{l\text{-}i}$ or S_l/S_i) and indene to styrene ($\xi_{i\text{-}s}$ or S_i/S_s) have been estimated and tend to be constant and graphically present a plateau between 500 and 600°C with respective values of (0.4-0.5) and (1.3-1.2), as shown in Figure 7. Although full peak deconvolution was constrained by instrumental sensitivity and spectral overlap, compound identification was achieved using a combination of retention time matching, Kovats retention indices, and spectral correlation with a mass spectral library. This approach, while semi-quantitative, allowed identification of the dominant pyro-products and enabled selectivity trend analysis across the tested temperature range.

The formation of limonene, a key target compound due to its industrial relevance as a monoterpene solvent and fuel additive, is mechanically attributed to the intramolecular cyclisation of isoprene radicals. These radicals are derived from the depolymerisation and β-scission of polyisoprene chains in NR, particularly under moderate heating conditions (400-500°C). This pathway is supported by a previous study by Mkhize et al. (2016) and is consistent with the prevalence of limonene observed at lower pyrolysis temperatures. However, at higher temperatures (>600°C), a significant decline in limonene selectivity ratio to isoprene (up to 0.7 at 70°C) was noted. This behaviour is attributed to secondary thermal transformations, including Diels-Alder rearrangements, dehydrogenation, and cracking reactions, which convert limonene into monoaromatic hydrocarbons such as toluene, xylene, and styrene. Xu et al. (2018) and Menares et al. (2020) have reported similar findings, demonstrating that limonene acts as a thermally labile intermediate whose ring structure opens or rearrang-

TABLE 3: Peak areas and selectivity of main compounds.

Compounds	Peak areas (%)				Selectivity (%)			
Temp. (°C)	400	500	600	700	400	500	600	700
Isoprene	10.21	16.81	13.52	11.67	27.1	37.6	35.2	36.6
Limonene	24.17	22.28	16.75	9.13	64.2	49.9	43.6	28.6
Styrene	1.17	1.86	1.89	2.97	3.1	4.2	4.9	9.3
Benzene	0.1	0.28	0.49	1.09	0.3	0.6	1.3	3.4
Toluene	0.97	1.35	2.85	3.06	2.6	3.0	7.4	9.6
Xylene	1.03	2.01	2.81	3.97	2.7	4.5	7.3	12.4
Indene		0.08	0.09		0.0	0.2	0.2	0.0
Total	37.65	44.67	38.4	31.89	100	100	100	100

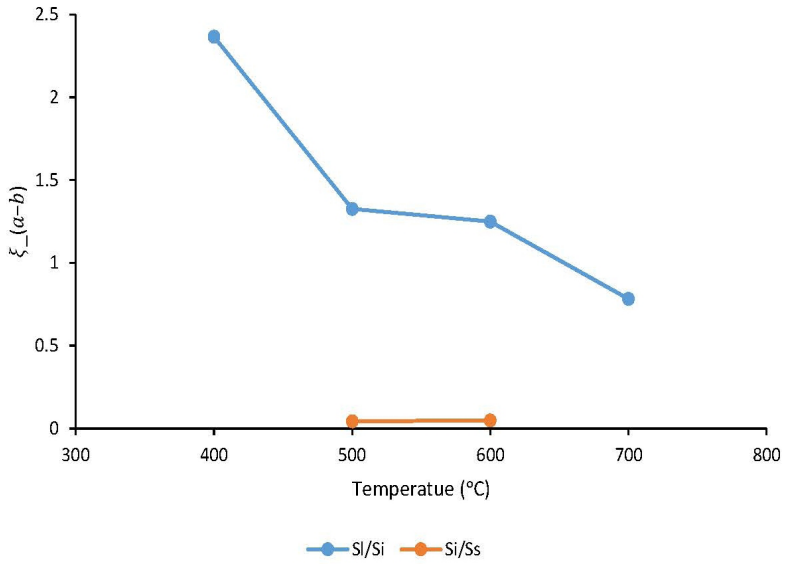

FIGURE 7: Relative formation of important compounds.

es under severe thermal steps, favouring aromatisation pathways.

Furthermore, the enhanced presence of monoaromatics and light hydrocarbons in the high-temperature chromatograms provides strong evidence of secondary degradation reactions, including the cracking of heavier terpenes and recombination of smaller radicals. These reactions shift the product spectrum from oxygenated or cyclic compounds to thermodynamically favoured aromatics and gases, aligning with the thermochemical principles of pyrolysis under kinetic versus thermodynamic control.

3.4.3 Heating rate influence on chemical influence

In a series of Evolved Gas Analysis experiments, the heating rate was varied from 20 to 50°C/min and 100°C/min at the obtained optimal temperature of 500°C.

The heating rate was found to have an influence on WTs pyrolysis kinetic parameters by increasing the activation energy and pre-exponential coefficient with an increase in the heating rate (Leung & Wang, 1998). Moreover, Mkhize et al. (2019) evidenced the effect of heating rate on isoprene and dl-limonene production. They reported that the reaction progress at peak dl-limonene increased as the heating rate was raised to higher values, up to 100°C/min. In this study, the heating rate has been increased and varied from 20 to 50°C/min, then 100°C/min for trend verification and confirmation. Figure 8 presents the selectivity to limonene formation at various heating rates.

The selectivity to limonene increases with the rise of heating rate, from around 30.8% at 20°C/min to 37.8% at 50°C/min. To confirm the observed trend, an experiment at a greater heating rate, i.e., 100°C/min, has been conducted and the selectivity to limonene continues to rise with the rise of heating rate values. Therefore, the heating rate plays a major role in the WTs pyrolysis for the formation of valuable products . From the above observations, limonene formation is favoured by high heating rates, as stated by Mkhize et al. (2019). The enhancement of limonene selectivity at higher heating rates can be attributed to two synergistic effects. First, rapid heating limits the residence time of primary volatile species in the hot zone, thereby suppressing secondary cracking and aromatisation reactions that typically degrade monoterpenes such as limonene into smaller or more stable aromatic compounds. Second, high heating rates accelerate the fragmentation of polyisoprene chains in natural rubber, increasing the formation of isoprene radicals. These radicals undergo intramolecular cyclisation to form Limone through a gas-phase mechanism, a process favoured kinetically under rapid thermal ramping conditions.

When benchmarked against recent studies, the limonene selectivity of 49.9% (peak-area) achieved in this work at 500°C is among the highest reported for thermal pyrolysis without added catalysts, while the 0.2% indene selectivity reflects its lower abundance but confirmed presence in the vapour-phase product spectrum. Menares et al. (2020) reported a comparable limonene peak area of ~51% at < 500°C using quasi-isothermal Py-GC/MS, though indene was not quantified. In fixed-bed pyrolysis, Mkhize et al. (2016) obtained a maximum limonene yield of 7.62 wt% of the oil fraction at 475°C, significantly lower than the present peak-area percentage, while their subsequent kinetic study quantified activation energies for limonene and isoprene but not indene. At pilot scale, Li et al., (2004) reported about 5.4 wt% limonene in the liquid fraction at 500°C, demonstrating the challenges of maintaining high selectivity during scale-up. These comparisons underscore the advantage of the hybrid TGA-Ty-GC/MS methodology in this work, which integrates kinetic analysis with compound-specific detection to achieve both low apparent activation energies (122-145 $kJ.mol^{-1}$) and high limonene selectivity under optimized conditions.

While the formation of limonene and indene is found to be favoured under specific pyrolysis conditions (500°C and 100°C/min), the commercial viability of their recovery also depends on the ease of downstream separation. Limonene, being a relatively volatile and thermally stable

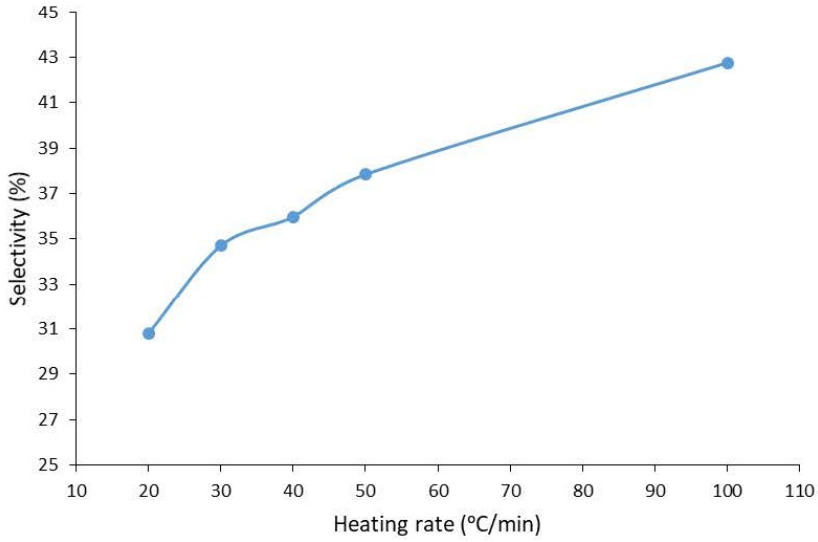

FIGURE 8: Selectivity to limonene formation.

monoterpene, can be efficiently separated via fractional condensation or distillation due to its distinct boiling point (~176°C) and low affinity for co-condensed char. Indene (boiling point ~181°C), though more prone to secondary polymerization, may also be recovered via low-temperature condensation or vacuum distillation techniques. A central difficulty arises from the close boiling points of limonene and indene, which can lead to co-elution in distillation and limit achievable purities without advanced separation measures. Furthermore, tyre pyrolysis oil contains a complex matrix of other mono- and polycyclic aromatics, some of which share similar volatility and molecular weight, complicating isolation. Multi-stage fractional distillation with high-efficiency packing can improve separation sharpness but increases capital and operational costs. Adsorption-based process using tailored sorbents such as modified zeolites or silica-alumina offers a means of selectively retaining aromatic compounds , enabling partial enrichment of limonene in the raffinate phase. Membrane-assisted pervaporation has also been explored for hydrocarbon mixtures, providing a potentially lower energy alternative that exploits molecular size and polarity differences (Smitha et al., 2004).

From a scale-up perspective, integration of these techniques into continuous pyrolysis systems must also consider fouling behaviour, regeneration of adsorbents or membranes, and the trade-off between purity and recovery efficiency. While high-purity limonene and indene markets could offer attractive revenue streams, the economic feasibility will depend on developing hybrid separation trains that combine condensation, adsorption, and membrane processes to achieve the necessary selectivity at a competitive cost. This underscores the need for further research into optimised separation pathways specifically tailored to tyre pyrolysis oils, incorporating not only thermodynamic and kinetic considerations but also material compatibility and process economics. Such studies would be instrumental in bridging the gap between laboratory-scale chemical yield optimisation and viable industrial-scale production.

4. CONCLUSIONS

This study investigated the pyrolysis behaviour of TT crumbs using integrated thermogravimetric analysis, kinetic modelling, and Py-GC/MS to understand the formation and selectivity of valuable compounds, notably limonene and indene. Model-free and model-fitting approaches revealed activation energy values ranging from 122 and 145 $kJ.mol^{-1}$ and identified key reaction zones associated with NR and SBR degradation. The process was best described by D2 and F2 kinetic models, indicating multi-step decomposition behaviour.

Product analysis showed that limonene formation peaked at moderate temperatures, with selectivity decreasing from 64.2% at 400°C to 28.6% at 700°C due to secondary reactions. Conversely, increasing the heating rate significantly enhanced limonene selectivity, rising from 30.8% at 20°C/min to 42.7% at 100°C/min. Based on these findings, optimal operating conditions for limonene production are identified as 500°C and 100°C/min, offering a practical benchmark for process optimisation.

The findings from this study offer important theoretical contributions by identifying reaction zones linked to the production of limonene and indene and providing activation energy profiles across conversion extents. Practically, the kinetic and selectivity data can inform the development of optimised pyrolysis protocols. High limonene yield at moderate temperature and fast heating rates suggests opportunities for targeted reactor control strategies to enhance the economic viability of tyre-derived oil recovery. Although this study does not include a process simulation or scale-up assessment, the kinetic parameters and product selectivity profiles generated herein provide a robust foundation for future modelling and design of industrial units targeting specific chemical yields. For instance, the identification of 500°C and 100°C/min as optimal conditions for limonene production can guide reactor temperature and residence time settings.

Limitations of this study include the use of tyre feedstock from a single source and the absence of a catalyst

or continuous reactor validation. Despite these constraints, the findings have direct implications for industrial scale-up and contribute to the development of tailored pyrolysis strategies aimed at chemical valorisation from end-of-life tyres.

Future research should explore the use of catalytic systems to enhance selectivity toward targeted chemicals like limonene and indene. The incorporation of zeolite-based catalysts, for instance, may provide shape-selective advantages and suppress unwanted side reactions. Additionally, transitioning to continuous pyrolysis systems with integrated vapour recovery and purification units would be essential for industrial implementation. Investigating solvent-assisted or membrane-based separation methods could also offer energy-efficient alternatives for post-processing.

REFERENCES

Aslan, D. I., Parthasarathy, P., Goldfarb, J. L., & Ceylan, S. (2017). Pyrolysis reaction models of waste tires: Application of Master-Plots method for energy conversion via devolatilization. Waste Management, 68, 405-411. https://doi.org/https://doi.org/10.1016/j.wasman.2017.06.006

Coats, A., & Redfern, J.-P. (1965). Kinetic parameters from thermogravimetric data. II. Journal of Polymer Science Part B: Polymer Letters, 3(11), 917-920. https://doi.org/https://doi.org/10.1002/pol.1965.110031106

Danon, B., & Görgens, J. (2015). Determining rubber composition of waste tyres using devolatilisation kinetics. Thermochimica Acta, 621, 56-60. https://doi.org/https://doi.org/10.1016/j.tca.2015.10.008

Danon, B., Mkhize, N., Van Der Gryp, P., & Görgens, J. (2015). Combined model-free and model-based devolatilisation kinetics of tyre rubbers. Thermochimica acta, 601, 45-53. https://doi.org/https://doi.org/10.1016/j.tca.2014.12.003

Ding, K., Zhong, Z., Zhang, B., Song, Z., & Qian, X. (2015). Pyrolysis characteristics of waste tire in an analytical pyrolyzer coupled with gas chromatography/mass spectrometry. Energy & Fuels, 29(5), 3181-3187. https://doi.org/https://doi.org/10.1021/acs.energyfuels.5b00247

Ding, K., Zhong, Z., Zhang, B., Wang, J., Min, A., & Ruan, R. (2016). Catalytic pyrolysis of waste tire to produce valuable aromatic hydrocarbons: an analytical Py-GC/MS study. Journal of Analytical and applied Pyrolysis, 122, 55-63. https://doi.org/https://doi.org/10.1016/j.jaap.2016.10.023

Doddipatla, S., Galimova, G. R., Wei, H., Thomas, A. M., He, C., Yang, Z., Morozov, A. N., Shingledecker, C. N., Mebel, A. M., & Kaiser, R. I. (2021). Low-temperature gas-phase formation of indene in the interstellar medium. Science advances, 7(1), eabd4044. https://doi.org/https://doi.org/10.1126/sciadv.abd4044

Friedman, H. L. (1964). Kinetics of thermal degradation of char-forming plastics from thermogravimetry. Application to a phenolic plastic. Journal of polymer science part C: polymer symposia,

Han, J., Li, W., Liu, D., Qin, L., Chen, W., & Xing, F. (2018). Pyrolysis characteristic and mechanism of waste tyre: A thermogravimetry-mass spectrometry analysis. Journal of Analytical and applied Pyrolysis, 129, 1-5. https://doi.org/https://doi.org/10.1016/j.jaap.2017.12.016

Han, J., Yao, X., Zhan, Y., Oh, S.-Y., Kim, L.-H., & Kim, H.-J. (2017). A method for estimating higher heating value of biomass-plastic fuel. Journal of the Energy Institute, 90(2), 331-335.

Iwarere, S. A., & Mkhize, N. M. (2019). PYROLYSIS OF VARIOUS TYRE TYPES: CHARACTERISTICS AND KINETIC STUDIES USING THERMOGRAVIMETRIC ANALYSIS. Detritus(2019-Volume), 0. https://doi.org/https://doi.org/10.31025/2611-4135/2019.13870

Khawam, A., & Flanagan, D. R. (2006). Basics and applications of solid-state kinetics: a pharmaceutical perspective. Journal of pharmaceutical sciences, 95(3), 472-498. https://doi.org/https://doi.org/10.1002/jps.20559

Kissinger, H. E. (1957). Reaction kinetics in differential thermal analysis. Analytical chemistry, 29(11), 1702-1706.

Leung, D., & Wang, C. (1998). Kinetic study of scrap tyre pyrolysis and combustion. Journal of Analytical and applied Pyrolysis, 45(2), 153-169. https://doi.org/https://doi.org/10.1016/S0165-2370(98)00065-5

Li, S.-Q., Yao, Q., Chi, Y., Yan, J.-H., & Cen, K.-F. (2004). Pilot-scale pyrolysis of scrap tires in a continuous rotary kiln reactor. Industrial & Engineering Chemistry Research, 43(17), 5133-5145. https://doi.org/https://doi.org/10.1021/ie030115m

Menares, T., Herrera, J., Romero, R., Osorio, P., & Arteaga-Pérez, L. E. (2020). Waste tires pyrolysis kinetics and reaction mechanisms explained by TGA and Py-GC/MS under kinetically-controlled regime. Waste Management, 102, 21-29. https://doi.org/https://doi.org/10.1016/j.wasman.2019.10.027

Mkhize, N., Danon, B., van der Gryp, P., & Görgens, J. (2019). Kinetic study of the effect of the heating rate on the waste tyre pyrolysis to maximise limonene production. Chemical Engineering Research and Design, 152, 363-371. https://doi.org/https://doi.org/10.1016/j.cherd.2019.09.036

Mkhize, N., van der Gryp, P., Danon, B., & Görgens, J. (2016). Effect of temperature and heating rate on limonene production from waste tyre pyrolysis. Journal of Analytical and applied Pyrolysis, 120, 314-320. https://doi.org/https://doi.org/10.1016/j.jaap.2016.04.019

Mwelwa, M. K., Iwarere, S. A., & Mkhize, N. M. (2023). Advances in understanding kinetic mechanisms underlying waste ground tyre rubber pyrolysis. Detritus(24), 52. https://doi.org/https://doi.org/10.31025/2611-4135/2023.18315

Ngxangxa, S. (2016). Development of GC-MS methods for the analysis of tyre pyrolysis oils [Thesis (MSc), Stellenbosch: Stellenbosch University]. http://hdl.handle.net/10019.1/98868

Quek, A., & Balasubramanian, R. (2012). Mathematical modeling of rubber tire pyrolysis. Journal of Analytical and applied Pyrolysis, 95, 1-13. https://doi.org/https://doi.org/10.1016/j.jhazmat.2008.11.034

Roy, C., & Unsworth, J. (1989). Pilot plant demonstration of used tyres vacuum pyrolysis. Pyrolysis and gasification, 180-189.

Seidelt, S., Müller-Hagedorn, M., & Bockhorn, H. (2006). Description of tire pyrolysis by thermal degradation behaviour of main components. Journal of analytical and applied pyrolysis, 75(1), 11-18. https://doi.org/https://doi.org/10.1016/j.jaap.2005.03.002

Smitha, B., Suhanya, D., Sridhar, S., & Ramakrishna, M. (2004). Separation of organic–organic mixtures by pervaporation—a review. Journal of Membrane Science, 241(1), 1-21. https://doi.org/https://doi.org/10.1016/j.memsci.2004.03.042

Starink, M. (2003). The determination of activation energy from linear heating rate experiments: a comparison of the accuracy of isoconversion methods. Thermochimica acta, 404(1-2), 163-176.

Torabian, A., Kazemian, H., Seifi, L., Bidhendi, G. N., Azimi, A. A., & Ghadiri, S. K. (2010). Removal of petroleum aromatic hydrocarbons by surfactant-modified natural zeolite: the effect of surfactant. CLEAN–Soil, Air, Water, 38(1), 77-83. https://doi.org/https://doi.org/10.1002/clen.200900157

Tsipa, P. C., Phiri, M. M., Iwarere, S. A., Mkhize, N. M., Phiri, M. J., & Hlangothi, S. P. (2024). A novel chemical pre-pyrolysis treatment of waste tyre crumbs: A viable way for low temperature waste tyre pyrolysis. Journal of analytical and applied pyrolysis, 181, 106631. https://doi.org/https://doi.org/10.1016/j.jaap.2024.106631

Venkatesh, M., Ravi, P., & Tewari, S. P. (2013). Isoconversional kinetic analysis of decomposition of nitroimidazoles: Friedman method vs Flynn–Wall–Ozawa method. The Journal of Physical Chemistry A, 117(40), 10162-10169. https://doi.org/https://doi.org/10.1021/jp407526r

Vyazovkin, S., Burnham, A. K., Criado, J. M., Pérez-Maqueda, L. A., Popescu, C., & Sbirrazzuoli, N. (2011). ICTAC Kinetics Committee recommendations for performing kinetic computations on thermal analysis data. Thermochimica acta, 520(1-2), 1-19. https://doi.org/https://doi.org/10.1016/j.tca.2011.03.034

Williams, P. T., & Besler, S. (1995). Pyrolysis-thermogravimetric analysis of tyres and tyre components. Fuel, 74(9), 1277-1283. https://doi.org/https://doi.org/10.1016/0016-2361(95)00083-H

Xu, F., Wang, B., Yang, D., Ming, X., Jiang, Y., Hao, J., Qiao, Y., & Tian, Y. (2018). TG-FTIR and Py-GC/MS study on pyrolysis mechanism and products distribution of waste bicycle tire. Energy Conversion and Management, 175, 288-297. https://doi.org/https://doi.org/10.1016/j.enconman.2018.09.013